Published in final edited form as:

Oncogene. 2016 March 3; 35(9): 1099–1110. doi:10.1038/onc.2015.163.

Stromal fibroblasts facilitate cancer cell invasion by a novel invadopodia-independent matrix degradation process

Hong Cao[#1,2], **Robbin D. Eppinga**[#1,3], **Gina L. Razidlo**[#1,2], **Eugene W. Krueger**[1], **Jing Chen**[1], **Li Qiang**[2], and **Mark A. McNiven**[1,2]

[1]Division of Gastroenterology and Hepatology, Mayo Clinic, Rochester, Minnesota USA

[2]Department of Biochemistry and Molecular Biology, Mayo Clinic, Rochester, Minnesota USA

[#] These authors contributed equally to this work.

Abstract

Metastatic invasion of tumors into peripheral tissues is known to rely upon protease-mediated degradation of the surrounding stroma. This remodeling process utilizes complex, actin-based, specializations of the plasma membrane termed invadopodia that act both to sequester and release matrix metalloproteinases. Here we report that cells of mesenchymal origin, including tumor-associated fibroblasts, degrade substantial amounts of surrounding matrix by a mechanism independent of conventional invadopodia. These degradative sites lack the punctate shape of conventional invadopodia to spread along the cell base and are reticular and/or fibrous in character. In marked contrast to invadopodia, this degradation does not require the action of Src kinase, Cdc42, or Dyn2. Rather, inhibition of Dyn2 causes a dramatic upregulation of stromal matrix degradation. Further, expression and activity of matrix metalloproteinases are differentially regulated between tumor cells and stromal fibroblasts. This matrix remodeling by fibroblasts increases the invasive capacity of tumor cells, thereby illustrating how the tumor microenvironment can contribute to metastasis. These findings provide evidence for a novel matrix remodeling process conducted by stromal fibroblasts that is substantially more effective than conventional invadopodia, distinct in structural organization, and regulated by disparate molecular mechanisms.

Keywords

invadopodia; matrix metalloproteinases; Dynamin 2; metastasis; cancer associated fibroblasts

To whom correspondence should be addressed: Mark A McNiven, Mayo Clinic, 200 First St. SW, Rochester, MN 55905, ; Email: mmcniven@mayo.edu, 507-284-0683, Fax: 507-284-2053

[3]Current Address: Department of Biology, Dordt College, Sioux Center, Iowa, USA

Conflict of interest:

The authors declare no conflict of interest.

Supplementary Information accompanies the paper on the Oncogene website (http://www.nature.com/onc).

Introduction

Dissemination of neoplastic cells away from the primary tumor is a characteristic of metastatic invasion and is a primary obstacle to the treatment of cancer. Invasion requires complex, agonist-activated, and actin-based tumor cell migration machinery that works in tandem with the secretion of matrix-remodeling metalloproteinases (MMPs). This secretion of matrix-degrading proteases is believed to be largely coordinated by complex organelles termed “invadopodia,” protrusions of the plasma membrane built upon a core of actin filaments and scores of associated proteins ([1]). Invadopodia assembly and function are regulated by multiple factors, including the signaling activity of Src kinase, the actin remodeling properties of Cdc42, and the GTPase function of Dynamin 2 ([2-5]).The mechanisms by which these structures are regulated, formed, and facilitate protease secretion and activation are critical, as attenuating invadopodia function could reduce tumor dissemination.

Importantly, many tumor cells do not form invadopodia in culture, do not degrade the surrounding matrix, and do not themselves secrete proteases, yet are able to disseminate and invade robustly. Many solid tumors, in particular pancreatic tumors, consist predominantly of supportive stromal cells, generating a complex tumor microenvironment ([6]). This population of surrounding stellate cells and/or cancer associated fibroblasts (CAFs) may actually provide a significant stromal remodeling capacity to lead the way for invasive tumor cells ([7]). However, the mechanisms of matrix remodeling by stromal cells are not well characterized. Recent studies have implicated the actin regulatory protein palladin in promoting invadopodia formation by CAFs to contribute to tumor cell invasion ([8, 9]). In addition, stromal degradation can be dramatically upregulated in fibroblasts by expression of oncogenic Src, and this podosome-like degradation requires the GTPase Dynamin 2 ([4, 10]). However, mechanisms underlying fibroblast-based matrix degradation without ectopic expression of active Src are not well defined, and it is not clear if invadopodia are the primary drivers of matrix remodeling in stromal fibroblasts.

To this end, we have compared the matrix-degrading machinery of human cancer cell lines with that of multiple mesenchymal-derived supportive cells, including CAFs, pancreatic stellate cells, and non-cancer associated fibroblasts. While tumor cells largely utilize invadopodial-based degradation, the matrix degradation by stromal cells is markedly different. Stromal cell matrix degradation is tubular/reticular in organization, and is regulated by different molecular machinery than invadopodial degradation by the tumor cells. These findings suggest that neoplastic epithelial cells and supportive stromal cells exhibit differential mechanisms to mediate matrix remodeling. The non-invadopodial degradation by CAFs in the tumor microenvironment could possess a substantial capacity to amplify the invasive properties of the tumor cells.

Results

Differential requirements for the large GTPase Dynamin in matrix degradation

To compare the degradative patterns between epithelial tumor cells and stromally-derived mesenchymal fibroblasts, cells were plated on fluorescent gelatin-coated coverslips and

allowed to degrade the gelatin matrix ([11]). Cell models included human adenocarcinoma cell lines of pancreatic (BxPC3, DanG) and breast (MDA-MB-231) origin, and several mesenchymal cell lines including human foreskin fibroblasts, rat and mouse fibroblasts, and three different pancreatic stromal cell lines: CAFs isolated from human pancreatic ductal adenocarcinoma (PDAC) patient-derived xenografts, and normal pancreatic stellate cells (PSC-1 and PSC-2), which are thought to be a primary source of CAFs in pancreatic cancers ([12]).

Epithelial tumor cells degraded the fluorescent substrate in a punctate pattern, representing conventional invadopodia (Fig. 1a-c), and showed substantial colocalization with the invadopodial markers actin and cortactin (Fig. 1j). In contrast, stromal fibroblasts and stellate cells displayed a combination of peripheral filamentous, focal adhesion-like degradation patterns ([13], [14]) and a series of elaborate tubular-reticular networks (Fig.1d-g), which showed no colocalization with actin or cortactin (Fig. 1k). These data suggest the matrix degradation accomplished by the fibroblasts and PSCs is distinct from the invadopodial matrix degradation of the tumor cells. All cells displayed a wide range of degradative activity as well as variations in the amount of matrix degraded per cell, with 90% of DanG and 35% of BxPC3 cells remodeling matrix, compared to just 25% of the human fibroblasts or <5% of the CAFs (Fig. 1h-i). Degradation by all cell types was completely inhibited by the MMP inhibitor BB-94, demonstrating that the degradation is protease-dependent (Supplementary Fig. S1). Interestingly, the area of degradation by the mesenchymal cells was notably higher than the BxPC3 or MDA-MB-231 tumor cells, which form bona fide invadopodia and are invasive (Fig. 1i). Therefore, this pattern of fibroblast-based matrix degradation is at least as potent as the degradation by tumor cells, if not more so.

To test if these different degradative phenotypes represent distinct mechanistic processes by epithelial versus mesenchymal cells, we tested the requirement for the large GTPase dynamin in the capacity to form invadopodia. The ubiquitous form of dynamin (Dyn2) is essential for the formation and function of invadopodia, presumably by mediating structural interactions between the ventral cell membrane and the actin cytoskeleton ([2], [10]). Indeed, siRNA-mediated knockdown of Dyn2 significantly reduced invadopodia formation and matrix degradation in the adenocarcinoma cell lines (Fig. 2a-j, x-y). In surprising contrast, the reduction of Dyn2 in the stromal cells caused a massive increase in matrix degradation, with a significant enlargement of the tubular-reticular patterns that extend from the cell center to the periphery. Knockdown of Dyn2 in stromal cells induced a 4-8 fold increase in the percent of cells degrading the matrix (Fig. 2l-x), as well as a striking 2-6 fold increase in the area of matrix degraded per cell (Fig. 2y).

To pursue the unexpected finding that fibroblasts degrade more matrix under conditions of low Dyn2 expression, we utilized MEFs from dynamin knockout mice ([15]). These cells have an inducible knockout of Dyn1 and Dyn2 driven by 4-hydroxy-tamoxifen (4HT). Similar to the human and rat fibroblasts (Fig. 2), the parental MEFs (DKO) exhibit very low levels of matrix degradation. Strikingly, 4HT-induced knockout of Dyn2 resulted in a massive increase in matrix degradation, with a 6-fold increase in the percent of cells capable of degrading matrix and a 10-fold increase in degradation area per cell, and the induction of the

massive reticular degradation pattern (Fig. 3a-c, f-g). This increase is ablated in the knockout cells re-expressing wild type Dyn2, but not GTPase defective Dyn2K44A (Fig. 3d-g). Similarly, overexpression of dominant negative Dyn2 K44A in rat fibroblasts induces the same dramatic matrix degradation, whereas expression of Dyn2 K44A in DanG tumor cells suppresses matrix degradation (Supplementary Fig. S2). Together, these data suggest that in fibroblasts, Dyn2 actually represses matrix degradation in a manner that requires its GTPase activity, a finding that is completely contrary to that observed in the epithelial-based tumor cells and contrary to the role of Dyn2 in the Src-induced, podosome-like degradation structures observed in mesenchymal cells ([2], [10]).

Fibroblast-derived ECM degradation is distinct from invadopodia-based degradation

The massive upregulation of matrix degradation by fibroblasts following depletion of Dyn2 does not resemble conventional invadopodia, raising the exciting possibility that these degradative structures are not only morphologically different from those in epithelial cells, but also mechanistically distinct. Invadopodial-based matrix degradation in tumor cells colocalizes with puncta positive for actin and cortactin, components of invadopodia. However, the sites of matrix degradation by the fibroblasts and PSCs showed no colocalization with actin or cortactin (Fig. 1, Supplemental Fig. 3). We hypothesized that the reticular degradation pattern actually represented the accumulated degradation of multiple dynamic invadopodia over time. To test this, matrix degradation was imaged at very early timepoints. Stromal cells were depleted of Dyn2 to amplify the nontraditional matrix degradation, then plated on fluorescent gelatin-coated coverslips in the presence of the MMP inhibitor BB-94. The BB-94 was then washed out, and cells were fixed and stained after 0-8 hours. Even within 1-2 hours, there was no colocalization between actin or cortactin with patterns of matrix degradation (Supplementary Fig. S3, Supplementary Movies 1-3), suggesting that the degradation is distinct from the canonical actin-based invadopodial machinery.

Src kinase activity induces invadopodia formation and maturation, and is required for invadopodial-based matrix degradation in tumor cells ([4], [16]). Consistent with this model, treatment of tumor cells with the Src inhibitor PP2 severely inhibited matrix degradation (Fig. 4a-d,i-j). We then tested the requirement for Src in fibroblast-based degradation. Using both DKO MEFs and rat fibroblasts, Dyn2 was depleted by tamoxifen treatment or siRNA to promote matrix degradation. The cells were then plated on the fluorescent gelatin substrate in the presence of PP2 or DMSO vehicle control. Surprisingly, PP2 treatment had no inhibitory effect on matrix degradation by fibroblasts, even at short timepoints (Fig. 4e-j, Supplementary Fig. S4), suggesting that Src activity is not required for this stromal-based matrix degradation. Similar results were observed in control fibroblasts without knockdown of Dyn2, which degrade matrix by a non-invadopodial mechanism but at a lower frequency (Supplementary Fig. S4). These findings further indicate that the degradation by the fibroblasts is mechanistically distinct from invadopodia.

The small GTPase Cdc42 is a well-characterized regulator of invadopodia formation ([3], [17], [18]). Indeed, expression of dominant negative Cdc42 (T17N) inhibited matrix degradation in the DanG tumor cells (Fig. 4k-l,o-p). Therefore, we tested if the large-scale matrix

degradation induced in fibroblasts required Cdc42 activity. DKO MEFs were treated with 4HT to induce dynamin knockout, were transfected with dominant negative Cdc42 (T17N), and were plated on the fluorescent gelatin substrate. Strikingly, dominant negative Cdc42 had no effect on matrix degradation in the dynamin-depleted fibroblasts (Fig. 4m-p), while it dramatically inhibited matrix degradation in epithelial tumor cells. These data indicate that the fibroblast-derived matrix degradation is independent of Cdc42. Thus, taken together, these findings demonstrate that fibroblasts are able to degrade the extracellular matrix by a novel mechanism distinct from invadopodia. This robust, large-scale degradation is independent of the invadopodial master regulators Src and Cdc42, does not have the typical invadopodial architecture and degradation pattern, and has an opposite requirement for Dyn2 compared to traditional invadopodia, thereby defining a unique mechanism of matrix degradation.

The trafficking of metalloproteinases differs in tumor cells versus stromal fibroblasts

Thus far, we have demonstrated an intriguing difference in the regulation of matrix degradation in fibroblasts versus epithelial-derived tumor cells. Depletion of Dyn2 in carcinoma cells inhibits invadopodia-based matrix degradation, whereas depletion of Dyn2 in fibroblasts results in a dramatic upregulation of invadopodia-independent matrix degradation. In an attempt to identify the differences underlying the distinct mechanisms of matrix degradation between the two cell types, we assayed for changes in MMP activity. Dyn2 was depleted using siRNA or 4HT-induced knockout in both fibroblasts (HF, RF, PSC, DKO MEFs) and epithelial-derived tumor cells (DanG, BxPC3, MDA-MB-231), and culture medium supernatants were analyzed by gelatin zymography. Notably, knockdown of Dyn2 in mesenchymal cells resulted in a significant upregulation of MMP-2 activity, while total levels of MMP-2 were not significantly altered (Fig. 5 a-b). In contrast, the epithelial-derived tumor cells had comparatively lower levels of active and total MMP-2, as determined by both zymography and immunoblotting, and no increase in MMP-2 activity was observed in the tumor cells. These data suggest that matrix degradation in epithelial tumors and mesenchymal fibroblasts are accomplished differently, and that fibroblast-mediated degradation may be regulated through MMP-2 activity, which in turn is modulated by Dyn2.

As total levels of MMP-2 protein were not significantly altered following Dyn2 knockdown, the data suggest that Dyn2 regulates activation of MMP-2. Pro-MMP-2 is cleaved and activated extracellularly by membrane-tethered MT1-MMP (membrane type 1-matrix metalloproteinase), a protease critical to invadopodia function and matrix degradation by tumor cells ([19], [20]). MT1-MMP surface retention is regulated by Dyn2 function in endocytosis ([21]). Therefore, we hypothesized that MT1-MMP was differentially regulated by Dyn2 in the fibroblasts and epithelial-derived cell types, thereby selectively activating MMP-2 and leading to the differential regulation of matrix degradation. To test this, total MT1-MMP levels were initially assessed by immunoblotting. In mesenchymal cells, knockdown of Dyn2 led to a modest 30-50% increase in total MT1-MMP levels. In contrast, in epithelial tumor cells, knockdown of Dyn2 led to a modest reduction (30-50%) in total MT1-MMP (Fig. 6a-b). As reduced levels of Dyn2 could restrict the endocytic internalization of the MT1 protease from invadopodia at the cell surface, leading to

increased matrix degradation, we next tested if the changes in total cellular levels of MT1 translated to altered protease levels at the plasma membrane. Immunofluorescence was used to probe for MT1-MMP on non-permeabilized cells, thereby detecting only MT1-MMP on the cell surface. In mesenchymal cells, there was a striking (2-3.5 fold) increase in surface MT1-MMP following depletion of Dyn2 (Fig. 6c-g). In contrast, in the epithelial-derived tumor cells, knockdown of Dyn2 caused no increase, or induced a modest reduction of MT1-MMP on the cell surface. MT1-MMP is a major regulator of matrix remodeling, as MT1-MMP colocalized with sites of matrix degradation by both tumor cells and fibroblasts (Fig. 6h-i). However, these data suggest that MT1-MMP expression and trafficking are differentially regulated by Dyn2 in different cell types, with Dyn2 positively regulating or not affecting MT1-MMP surface expression in epithelial tumor cells, which form invadopodia, and Dyn2 negatively regulating MT1-MMP surface expression in mesenchymal cells, which degrade the ECM by an invadopodia-independent mechanism.

Of note, the distinct types of matrix degradation accomplished by tumor cells versus stromal fibroblasts were not attributed to an endocytic block alone, as inhibiting endocytosis by siRNA-mediated knockdown of clathrin exacerbated both the invadopodia-based matrix degradation of tumor cells, and the reticular, non-invadopodial degradation of fibroblasts, and also induced a distinct, fibrous pattern of degradation by the PSC-2 cells (Fig. 6j-q). Therefore, while clathrin-mediated endocytosis contributes to matrix degradation in different cell types, presumably due to internalization and clearance of the degradative machinery, it is not the sole factor that distinguishes between the alternate degradative pathways.

The findings in Fig. 5 suggested that the upregulation of degradation by the stromal cells was mediated by an increase in MMP-2 activity. While depletion of Dyn2 in fibroblasts led to a dramatic increase in matrix degradation, as described above, this was completely prevented by knockdown of MMP-2 (Fig. 7a-h), suggesting that MMP-2 is indeed required for stromal matrix degradation. Similarly, siRNA-mediated knockdown of MT1-MMP resulted in a loss of MMP-2 activity (Fig. 7b), and also blocked matrix degradation in the Dyn2 knockdown cells, demonstrating that both proteases are required for this large-scale, invadopodia-independent matrix degradation (Fig. 7a-h). In contrast, whereas depletion of MT1-MMP in DanG tumor cells completely blocked matrix degradation, knockdown of MMP-2 had less of an effect (Fig. 7i-p). Similarly, treatment of fibroblasts with the MMP-2/MMP-9 inhibitor SB-3CT completely blocked the matrix degradation amplified by loss of Dyn2, but had less of an effect on DanG tumor cells (Supplementary Fig. S5). These data support a model by which MT1-MMP is a major activator of matrix degradation by both stromal cells and tumor cells, but that stromal cell degradation is mediated through MMP-2, whereas tumor cell degradation is less dependent upon MMP-2. Further, MMP-2 activation appears to distinguish the tubular/reticular degradation of mesenchymal cells from the punctate, MMP-2-independent, invadopodial degradations made by epithelial tumor cells (Fig. 7n).

Fibroblast-based matrix degradation promotes invasion by pancreatic tumor cells

Our findings indicate that fibroblasts can degrade the extracellular matrix by a novel mechanism that is distinct from tumor-associated invadopodia. In the context of the tumor

microenvironment, it is hypothesized that cross-talk between the tumor cells and stromal cells primes tumor cells for metastasis, with the fibroblasts creating a permissive environment that promotes invasion. One model is that the stromal cells contribute to tumor cell invasion by degrading and remodeling the extracellular matrix to allow tumor cell escape. Therefore, we tested if the fibroblast-based matrix degradation could support invasion by tumor cells *in vitro* using a co-culture model system.

PANC1 pancreatic tumor cells, which do not degrade a gelatin matrix, show minimal invasion through a gelatin-coated transwell membrane. We tested if providing stromal cells to degrade the matrix could promote PANC1 cell invasion. To this end, PANC1 cells were co-cultured with the stromal fibroblasts described above, and the resulting transwell invasion by PANC1 cells was quantified. Rat fibroblasts or CAFs were depleted of Dyn2 by siRNA, and then were co-cultured in a transwell invasion assay with PANC1 cells (Fig. 8e). When plated together, PANC1 cells were able to invade across a gelatin-coated transwell filter. Strikingly, depletion of Dyn2 in the fibroblasts, which induces matrix degradation, resulted in a marked upregulation of PANC1 invasion. Similar results were observed using DKO fibroblasts that were incubated with or without 4HT to induce Dyn2 knockout (Fig. 8a-d,f). The transwell invasion was inhibited by the MMP inhibitor BB-94, demonstrating that the invasion is dependent upon MMP activity and matrix degradation, and suggesting that the matrix-degrading capacity of the stromal fibroblasts promotes the transwell invasion of the tumor cells.

In line with these observations, co-culture with tumor cells capable of degrading the matrix should also promote the invasion of the PANC1 tumor cells. Indeed, co-culture with DanG cells, which exhibit potent matrix degradation, dramatically increased the transwell invasion of the PANC1 cells. In contrast to the stromal fibroblasts, siRNA-mediated depletion of Dyn2 in the DanG cells completely suppressed the induced invasion, consistent with the inhibitory effect on matrix degradation (Fig. 8g, Fig. 2). These data demonstrate that the invadopodia-independent matrix degradation inducible in fibroblasts is capable of promoting invasion of co-cultured tumor cells, and defines a novel mechanism by which fibroblast-tumor cell interactions in the tumor microenvironment could contribute to metastasis.

Discussion

Complex interactions between tumor cells and neighboring stromal cells regulate tumor progression and metastasis. In a mutualistic interaction, tumor cells activate adjacent fibroblasts, which then are primed both to remodel the extracellular matrix and secrete trans-acting factors to regulate the tumor cells. It has been proposed that CAFs can also secrete matrix-degrading proteases that could allow for the escape of tumor cells from the primary tumor. While tumor cells often degrade the matrix through the formation of specialized protrusions called invadopodia, in contrast, here we report a distinct mechanism of matrix degradation by fibroblasts regulated by the activity of the large GTPase Dyn2. This degradation is independent of invadopodia, as it exhibits a distinct pattern of degradation, does not require the activity of the kinase Src or the GTPase Cdc42, and is actually repressed, rather than supported, by the action of Dyn2. This novel form of matrix

degradation can support invasion by tumor cells, indicating a new mechanism by which stromal fibroblasts can promote tumor cell invasion.

CAFs have been extensively described as tumor-promoting, although their ablation also contributes to enhanced tumor growth and progression ([22], [23]), indicating a complex relationship between CAFs and tumor cells *in vivo*. CAFs promote tumor progression through secretion of cytokines and growth factors that stimulate tumor cell growth and migration, through maintenance of cancer stem cell properties, and by contributing to tumor cell metabolism ([12], [24-29]). In addition, CAFs have been implicated as direct regulators of tumor cell migration through mechanical regulation or serving as "leader" cells ([7], [30]). In this manuscript, we focus on the matrix-remodeling contribution of fibroblasts from both normal and neoplastic tissue. This matrix remodeling is highly relevant to multiple pathological settings such as fibrosis and wound healing, and is also able to promote tumor cell invasion *in vitro* (Fig. 8), demonstrating a significance during metastasis.

What is the structural basis of this invadopodia-independent matrix degradation in stromal fibroblasts? The pattern of degradation is reticular, suggesting a "tethering" of the proteases by cytoskeletal elements, yet we observed no obvious colocalization with a variety of cytoskeletal and organelle markers such as actin, cortactin, tubulin, the Golgi protein GM130, clathrin, or focal adhesion markers (Fig. 1, Supplementary Fig. S2, and data not shown). Our data suggest that this degradation is due to increased surface expression of MT1-MMP and increased activity of MMP-2, a secreted protease. However, the degradation is clearly focal, suggesting that the degradation is still associated with the membrane or a membrane-associated structure, and not just a result of excess soluble protease. Of note is the copious amount of matrix degradation induced in the fibroblasts in a short timeframe, compared to modest, punctate degradation originating from invadopodia (Figs. 1,2). While localized invadopodial degradation may be useful at the tip of an invading tumor cell to sense or degrade its local environment, the findings presented here raise the intriguing possibility that this novel type of fibroblast-derived matrix degradation may be important for large-scale matrix remodeling or invasion.

What molecular mechanisms account for the differences in matrix degradation between stromal and epithelial-derived tumor cells? Our data indicate that Dyn2 differentially regulates MMP-2 activity (Fig. 5), likely through surface expression of MT1-MMP. In fibroblasts, depletion of Dyn2 results in increased MT1-MMP at the cell surface (Fig. 6), consistent with the model that Dyn2 may be required for MT1-MMP endocytosis and internalization ([21]). Increased MT1-MMP at the surface would be available to activate extracellular MMP-2, which is increased in fibroblasts. However, inhibition of endocytosis by clathrin knockdown does not always phenocopy loss of Dyn2, particularly in epithelial tumor cells (Fig. 6). It is surprising that Dyn2 has these differential effects on MT1-MMP surface expression between the two cell types, and it will be important to determine how either MT1-MMP and/or Dyn2 are differentially regulated between mesenchymal and epithelial-derived cells.

How would this large-scale, invadopodia-independent degradation be induced in the context of human tumors? Fibroblast-derived matrix degradation was upregulated in this study by

depletion of Dyn2, which was used as a tool to manipulate signaling pathways and reveal a unique mechanism of degradation. While it is possible that Dyn2 expression is lost in CAFs, it is more likely that Dyn2-regulated signaling pathways could be altered in CAFs, such as endocytic or endosomal trafficking, or Dyn2-regulated cytoskeletal networks. Importantly, the differential regulation of matrix remodeling between tumor and stromal cells will increase the complexity of designing therapies to block tumor cell invasion. Inhibitors targeting classical invadopodial-based matrix degradation in tumor cells would not inhibit the large-scale matrix degradation inducible in fibroblasts, and could actually potentiate it, as in the case of Dyn2 depletion. These findings underscore the importance of defining the contributions of diverse cell types in the tumor microenvironment, and in understanding the basic cell biology underlying the mechanisms of invasion and migration in distinct cell types.

MATERIALS AND METHODS

Cell culture and transfection

BxPC-3 cells (ATCC CRL-1687), were maintained in RPMI-1640 medium with 10% fetal bovine serum (FBS) (Sigma, St. Louis, MN), 100 U/ml penicillin (P), and 100 mg/ml streptomycin (S) (Life Technologies, Carlsbad, CA). Human foreskin fibroblasts (HF, ATCC CRL-110), were maintained in MEM medium with 10% FBS and P/S. The following cell lines were maintained in DMEM medium with 10% FBS and P/S: PANC-1 (ATCC CRL-1469); DanG (provided by Dr. Martin Fernandez-Zapico, Mayo Clinic, Rochester, MN); MDA-MB-231 (ATCC HTB-26); rat fibroblasts (RF, ATCC CRL-1213); CAF cells (human cancer-associated fibroblasts, provided by Dr. Mark Truty, Mayo Clinic, Rochester, MN); human pancreatic stellate cells (PSC-1 provided by Dr. Debabrata Mukhopadhyay, Mayo Clinic, Rochester, MN; PSC-2 from ScienCell, Carlsbad, CA); and DKO (Dynamin conditional knockout fibroblasts, provided by Dr. Pietro De Camilli, Yale University, New Haven, CT, ([15])). Dynamin 1/2 knockout was induced by treatment with 2 μM 4-hydroxy-tamoxifen for 4-5 days. All cells were maintained in 5% CO_2 at 37°C. Inhibitors used were: MMP inhibitor BB-94 (2 μM, Tocris Bioscience, Bristol, UK), Src inhibitor PP2 (Calbiotech, Spring Valley, CA), or the MMP-2/MMP- 9 inhibitor SB-3CT (14 nM, Sigma, St. Louis, MO).

Cells were transfected with plasmid DNA using Lipofectamine 2000 and with siRNA using Lipofectamine RNAiMAX (Life Technologies) according to the manufacturer's instructions.

GFP-tagged and untagged Dyn2(aa) WT and K44A were described previously ([31-34]). Flag-tagged human Cdc42 T17N was provided by Dan Billadeau (Mayo Clinic, Rochester, MN). Myc-tagged human Cdc42 T17N was from Addgene (Addgene plasmid 12973, provided by Gary Bokoch).

Non-targeting siRNA and all targeting siRNAs were from Dharmacon (GE Healthcare): Human MMP-14 (MT1-MMP, #D-004145-02-0010); Dyn2 (Rat: D-080140-02, Human: D-004007-02) ([35]); MMP-2 (5'-GGAGAGCUGCAACCUGUUU-3') ([36]); Clathrin (#D-004001-02-0050).

Immunoblotting

For western blotting, cells were lysed in NP-40 lysis buffer (20 mM Tris-Cl, pH 8.0, 137 mM NaCl, 10% glycerol, 1% NP-40, 2 mM EDTA, Complete protease inhibitors (Roche)), and immunoblotted as described ([32]). Primary antibodies were: MT1-MMP (Epitomics, Burlingame, CA); MMP-2 (EP1183Y, Abcam, Cambridge, MA) and (H-76:sc-10736, Santa Cruz Biotechnology, Dallas, TX), cortactin (4F11, EMD Millipore, Billerica, MA), Dyn2 ([37]), and actin (Sigma). Horseradish peroxidase (HRP)-conjugated secondary antibodies were from Bio-source International (Camarillo, CA). Membranes were developed with enhanced chemiluminescence (Pierce) and were exposed to autoradiographic film (Eastman Kodak, Rochester, NY) to detect HRP.

Gelatin Zymography

Cells were cultured in the absence of serum for 24 hours. The culture medium was then collected and centrifuged for 2 min at 6000 rpm, then combined with zymogram sample buffer (BioRad, Hercules, CA), and incubated at room temperature for 10 minutes. Samples were resolved on a 7.5% SDS-PAGE gel containing 1 mg/ml gelatin. The gel was then incubated in 2.5% Triton X-100 at room temperature for 40 minutes with shaking, and rinsed with incubation buffer (50 mM Tris-B pH8.0; 150 mM NaCl; 10 mM CaCl; 0.05% NaN_3), then soaked in incubation buffer at 37°C for 20~24 hours in a shaking waterbath. The gel was then rinsed three times with dH2O, stained with Coomassie blue for 40 minutes at room temperature, and destained at room temperature for 2 hours.

Fluorescent Gelatin Degradation Assay

Gelatin-coated coverslips were prepared as described using Oregon green 488-labeled gelatin (Life Technologies) at a 1:8 ratio with unlabeled gelatin ([11]). Cells were plated on gelatin-coated coverslips and incubated for 8 hours. Alternatively, cells were incubated overnight in the presence of 2 μM BB-94 (Tocris). The following day, BB-94 was washed out and the cells were incubated for 8 hours before fixation and staining.

Cell Invasion Assay

Polycarbonate membranes (NeuroProbe, Inc., Gaithersburg, MD) containing 8 μm pores were coated with 0.3% gelatin and assembled into Blind Well Chambers (NeuroProbe, Inc.). PANC-1 were stably transduced with a lentivirus to express mDsRed ([35]), and were mixed with the indicated cell types in low-serum media (0.2% FBS). 1×10^5 PANC1 and 2×10^4 stromal cells were plated into the top chamber. The lower chamber contained DMEM with 10% FBS. After 8 hours, the cells were removed from the top of the filter, and the filters were fixed with formaldehyde, stained with DAPI and FITC-Phalloidin (Sigma), and imaged by fluorescence microscopy. Cells were scored as invaded if the nucleus had crossed the filter. The number of PANC1 cells on the bottom of the filter was counted in 4-5 10× fields per filter.

Immunofluorescence and Microscopy

Cells were prepared for immunofluorescence as described previously ([32]). Cells were incubated in primary antibodies for 2 h at 37°C (myc or FLAG polyclonal, Cell Signaling

Technologies; Dyn2 ([37]); MT1-MMP, Epitomics), washed with D-PBS, and incubated in labeled secondary antibody (Life Technologies) for 1 h at 37°C. Actin was stained using TRITC-Phalloidin (Sigma). The coverslips were mounted on glass slides using ProLong mounting medium (Molecular Probes, Life Technologies), and cells were imaged with an AxioObserver D.1 epifluorescence microscope (Carl Zeiss, Thornwood, NY) equipped with a 100-W mercury lamp using a 63×, 1.4 N.A. objective lens. Matrix degradation was visualized as a loss of Oregon green fluorescence on the labeled gelatin substrate. Contrast and intensity for each image were manipulated uniformly using Adobe Photoshop software. Images were analyzed with IVision software (BioVision, Mountain View, CA) ([32]).

Supplementary Material

Refer to Web version on PubMed Central for supplementary material.

Acknowledgements

This work was supported by R01 CA104125 to M.A.M. and P30DK084567 (Mayo Clinic Center for Cell Signaling in Gastroenterology). T32 DK007198 (to R.D.E.), and P50 CA102701 (Mayo Clinic SPORE in Pancreatic Cancer, to G.L.R.).

References

1. Murphy DA, Courtneidge SA. The ‘ins’ and ‘outs’ of podosomes and invadopodia: characteristics, formation and function. Nat Rev Mol Cell Biol. Jul; 2011 12(7):413–26. [PubMed: 21697900]
2. Baldassarre M, Pompeo A, Beznoussenko G, Castaldi C, Cortellino S, McNiven MA, et al. Dynamin participates in focal extracellular matrix degradation by invasive cells. Mol Biol Cell. Mar; 2003 14(3):1074–84. [PubMed: 12631724]
3. Yamaguchi H, Lorenz M, Kempiak S, Sarmiento C, Coniglio S, Symons M, et al. Molecular mechanisms of invadopodium formation: the role of the N-WASP-Arp2/3 complex pathway and cofilin. J Cell Biol. Jan 31; 2005 168(3):441–52. [PubMed: 15684033]
4. Chen WT, Chen JM, Parsons SJ, Parsons JT. Local degradation of fibronectin at sites of expression of the transforming gene product pp60src. Nature. Jul 11-17; 1985 316(6024):156–8. [PubMed: 2989711]
5. Buccione R, Orth JD, McNiven MA. Foot and mouth: podosomes, invadopodia and circular dorsal ruffles. Nat Rev Mol Cell Biol. Aug; 2004 5(8):647–57. [PubMed: 15366708]
6. Waghray M, Yalamanchili M, di Magliano MP, Simeone DM. Deciphering the role of stroma in pancreatic cancer. Curr Opin Gastroenterol. Sep; 2013 29(5):537–43. [PubMed: 23892539]
7. Gaggioli C, Hooper S, Hidalgo-Carcedo C, Grosse R, Marshall JF, Harrington K, et al. Fibroblast-led collective invasion of carcinoma cells with differing roles for RhoGTPases in leading and following cells. Nat Cell Biol. Dec; 2007 9(12):1392–400. [PubMed: 18037882]
8. Brentnall TA, Lai LA, Coleman J, Bronner MP, Pan S, Chen R. Arousal of cancer-associated stroma: overexpression of palladin activates fibroblasts to promote tumor invasion. PLoS One. 2012; 7(1):e30219. [PubMed: 22291919]
9. Goicoechea SM, Garcia-Mata R, Staub J, Valdivia A, Sharek L, McCulloch CG, et al. Palladin promotes invasion of pancreatic cancer cells by enhancing invadopodia formation in cancer-associated fibroblasts. Oncogene. Mar 6; 2014 33(10):1265–73. [PubMed: 23524582]
10. Destaing O, Ferguson SM, Grichine A, Oddou C, De Camilli P, Albiges-Rizo C, et al. Essential function of dynamin in the invasive properties and actin architecture of v-Src induced podosomes/invadosomes. PLoS One. 2013; 8(12):e77956. [PubMed: 24348990]
11. Artym VV, Zhang Y, Seillier-Moiseiwitsch F, Yamada KM, Mueller SC. Dynamic interactions of cortactin and membrane type 1 matrix metalloproteinase at invadopodia: defining the stages of

invadopodia formation and function. Cancer Res. Mar 15; 2006 66(6):3034–43. [PubMed: 16540652]

12. Ohlund D, Elyada E, Tuveson D. Fibroblast heterogeneity in the cancer wound. J Exp Med. Jul 28; 2014 211(8):1503–23. [PubMed: 25071162]
13. Wang Y, McNiven MA. Invasive matrix degradation at focal adhesions occurs via protease recruitment by a FAK-p130Cas complex. J Cell Biol. Feb 6; 2012 196(3):375–85. [PubMed: 22291036]
14. Yu X, Zech T, McDonald L, Gonzalez EG, Li A, Macpherson I, et al. N-WASP coordinates the delivery and F-actin-mediated capture of MT1-MMP at invasive pseudopods. J Cell Biol. Oct 29; 2012 199(3):527–44. [PubMed: 23091069]
15. Ferguson SM, Raimondi A, Paradise S, Shen H, Mesaki K, Ferguson A, et al. Coordinated actions of actin and BAR proteins upstream of dynamin at endocytic clathrin-coated pits. Dev Cell. Dec; 2009 17(6):811–22. [PubMed: 20059951]
16. Boateng LR, Huttenlocher A. Spatiotemporal regulation of Src and its substrates at invadosomes. Eur J Cell Biol. Nov-Dec;2012 91(11-12):878–88. [PubMed: 22823952]
17. Nakahara H, Otani T, Sasaki T, Miura Y, Takai Y, Kogo M. Involvement of Cdc42 and Rac small G proteins in invadopodia formation of RPMI7951 cells. Genes Cells. Dec; 2003 8(12):1019–27. [PubMed: 14750956]
18. Razidlo GL, Schroeder B, Chen J, Billadeau DD, McNiven MA. Vav1 as a central regulator of invadopodia assembly. Curr Biol. Jan 6; 2014 24(1):86–93. [PubMed: 24332539]
19. Sato H, Takino T, Kinoshita T, Imai K, Okada Y, Stetler Stevenson WG, et al. Cell surface binding and activation of gelatinase A induced by expression of membrane-type-1-matrix metalloproteinase (MT1-MMP). FEBS Lett. May 6; 1996 385(3):238–40. [PubMed: 8647259]
20. Okada A, Tomasetto C, Lutz Y, Bellocq JP, Rio MC, Basset P. Expression of matrix metalloproteinases during rat skin wound healing: evidence that membrane type-1 matrix metalloproteinase is a stromal activator of pro-gelatinase A. J Cell Biol. Apr 7; 1997 137(1):67–77. [PubMed: 9105037]
21. Jiang A, Lehti K, Wang X, Weiss SJ, Keski-Oja J, Pei D. Regulation of membrane-type matrix metalloproteinase 1 activity by dynamin-mediated endocytosis. Proc Natl Acad Sci U S A. Nov 20; 2001 98(24):13693–8. [PubMed: 11698655]
22. Rhim AD, Oberstein PE, Thomas DH, Mirek ET, Palermo CF, Sastra SA, et al. Stromal elements act to restrain, rather than support, pancreatic ductal adenocarcinoma. Cancer Cell. Jun 16; 2014 25(6):735–47. [PubMed: 24856585]
23. Ozdemir BC, Pentcheva-Hoang T, Carstens JL, Zheng X, Wu CC, Simpson TR, et al. Depletion of carcinoma-associated fibroblasts and fibrosis induces immunosuppression and accelerates pancreas cancer with reduced survival. Cancer Cell. Jun 16; 2014 25(6):719–34. [PubMed: 24856586]
24. Martinez-Outschoorn UE, Lisanti MP, Sotgia F. Catabolic cancer-associated fibroblasts transfer energy and biomass to anabolic cancer cells, fueling tumor growth. Semin Cancer Biol. Apr.2014 25:47–60. [PubMed: 24486645]
25. Egeblad M, Littlepage LE, Werb Z. The fibroblastic coconspirator in cancer progression. Cold Spring Harb Symp Quant Biol. 2005; 70:383–8. [PubMed: 16869775]
26. Calon A, Tauriello DV, Batlle E. TGF-beta in CAF-mediated tumor growth and metastasis. Semin Cancer Biol. Apr.2014 25:15–22. [PubMed: 24412104]
27. Mishra P, Banerjee D, Ben-Baruch A. Chemokines at the crossroads of tumor-fibroblast interactions that promote malignancy. J Leukoc Biol. Jan; 2011 89(1):31–9. [PubMed: 20628066]
28. Luga V, Wrana JL. Tumor-stroma interaction: Revealing fibroblast-secreted exosomes as potent regulators of Wnt-planar cell polarity signaling in cancer metastasis. Cancer Res. Dec 1; 2013 73(23):6843–7. [PubMed: 24265274]
29. De Wever O, Van Bockstal M, Mareel M, Hendrix A, Bracke M. Carcinoma-associated fibroblasts provide operational flexibility in metastasis. Semin Cancer Biol. Apr.2014 25:33–46. [PubMed: 24406210]

30. Karagiannis GS, Poutahidis T, Erdman SE, Kirsch R, Riddell RH, Diamandis EP. Cancer-associated fibroblasts drive the progression of metastasis through both paracrine and mechanical pressure on cancer tissue. Mol Cancer Res. Nov; 2012 10(11):1403–18. [PubMed: 23024188]

31. Cao H, Orth JD, Chen J, Weller SG, Heuser JE, McNiven MA. Cortactin is a component of clathrin-coated pits and participates in receptor-mediated endocytosis. Mol Cell Biol. Mar; 2003 23(6):2162–70. [PubMed: 12612086]

32. Cao H, Garcia F, McNiven MA. Differential distribution of dynamin isoforms in mammalian cells. Mol Biol Cell. Sep; 1998 9(9):2595–609. [PubMed: 9725914]

33. Cao H, Thompson HM, Krueger EW, McNiven MA. Disruption of Golgi structure and function in mammalian cells expressing a mutant dynamin. J Cell Sci. Jun; 2000 113(Pt 11):1993–2002. [PubMed: 10806110]

34. McNiven MA, Kim L, Krueger EW, Orth JD, Cao H, Wong TW. Regulated interactions between dynamin and the actin-binding protein cortactin modulate cell shape. J Cell Biol. Oct 2; 2000 151(1):187–98. [PubMed: 11018064]

35. Eppinga RD, Krueger EW, Weller SG, Zhang L, Cao H, McNiven MA. Increased expression of the large GTPase dynamin 2 potentiates metastatic migration and invasion of pancreatic ductal carcinoma. Oncogene. Mar 8; 2012 31(10):1228–41. [PubMed: 21841817]

36. Ries C, Egea V, Karow M, Kolb H, Jochum M, Neth P. MMP-2, MT1-MMP, and TIMP-2 are essential for the invasive capacity of human mesenchymal stem cells: differential regulation by inflammatory cytokines. Blood. May 1; 2007 109(9):4055–63. [PubMed: 17197427]

37. Henley JR, Krueger EW, Oswald BJ, McNiven MA. Dynamin-mediated internalization of caveolae. J Cell Biol. Apr 6; 1998 141(1):85–99. [PubMed: 9531550]

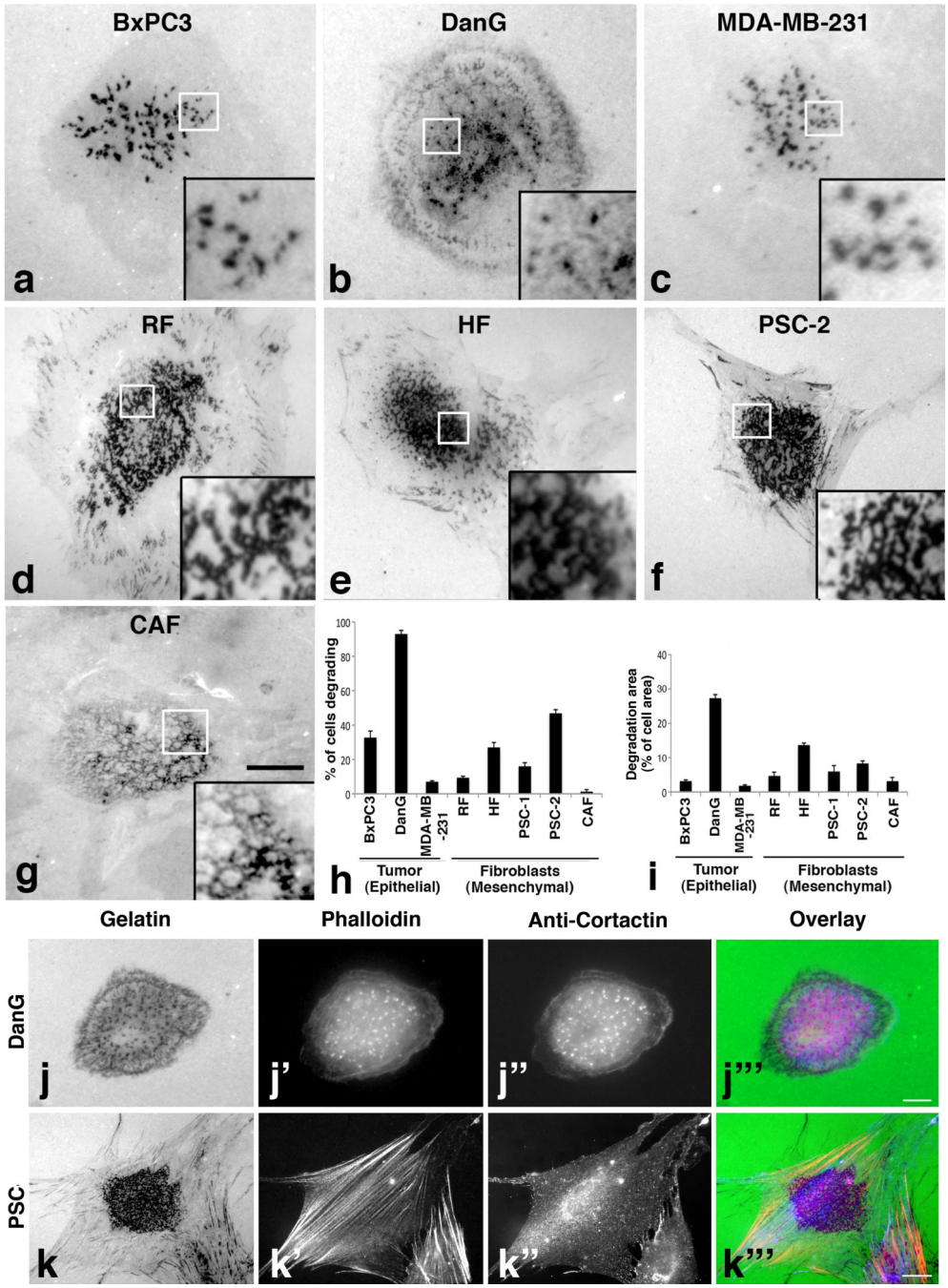

Figure 1. Epithelial tumor cells and stromal cells exhibit distinct patterns of matrix degradation

Multiple different epithelial-derived tumor cells and mesenchymal cell types were plated on a fluorescent gelatin substrate and cultured for 8 hours prior to fixation. (a-c) The pancreatic tumor cells BxPC3 and DanG, and breast cancer cell line MDA-MB-231, show largely punctate, invadopodial-like degradation patterns. (d-g) Fibroblasts and stellate cells exhibit a unique pattern of centrally positioned, reticular matrix degradation. Boxed regions are magnified in insets. (h) Graph depicting the percentage of each cell type that degrades matrix after 8 hours. Graphed results represent the mean +/− S.D. of >100 cells in each of

three independent experiments. (i) Of the cells that degraded the matrix, the area of degradation was quantified and normalized to the total cell area. Graphed results represent the mean +/− S.D. of 10 cells in each of three independent experiments. (j) Matrix degradation by DanG cells colocalizes with actin and cortactin, indicating the presence of functional invadopodia. (k) In contrast, matrix degradation by PSCs shows no colocalization with actin or cortactin. RF: rat fibroblasts, HF: human fibroblasts, PSC: pancreatic stellate cells, CAF: cancer associated fibroblasts. Scale bar, 10 μm.

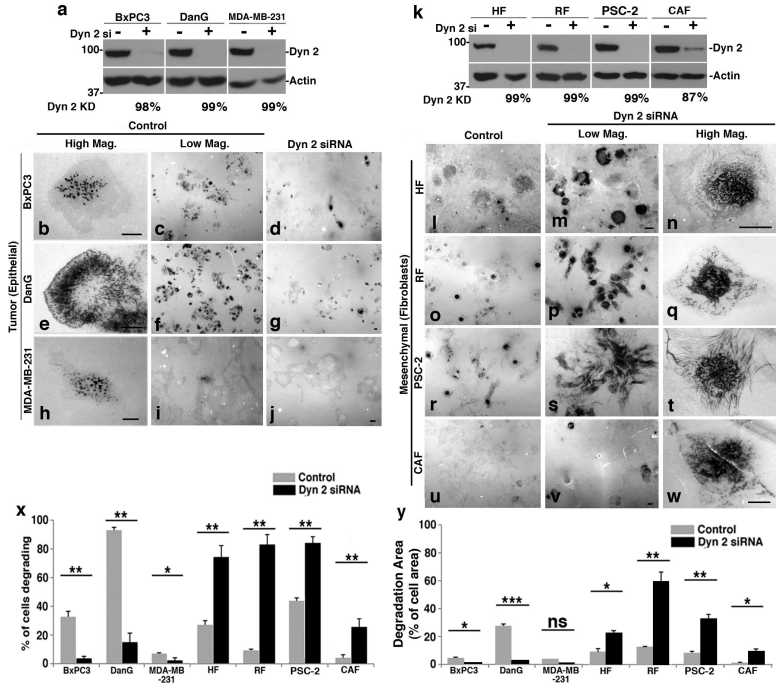

Figure 2. Reduction of Dynamin 2 induces a differential response in matrix degradation between tumor and mesenchymal cells

(a-j) Dyn2 was depleted by siRNA in DanG, BxPC3, or MDA-MB-231 tumor cells, and cells were then plated on a fluorescent gelatin substrate. (a) Knockdown was confirmed by immunoblotting. The percent of the Dyn2 knockdown is indicated under the blot. (b-j) Tumor cells that spontaneously degrade matrix via invadopodia are markedly inhibited in their degradative capacity by Dyn2 knockdown. (k-w) Dyn2 was depleted by siRNA in RF, HF, and PSC-2, and cells were then plated on a fluorescent gelatin matrix. In contrast to the tumor cells, mesenchymal fibroblastic cells that normally exhibit modest amounts of degradation show increased matrix remodeling by 4-5-fold upon reduction of Dyn2. Most degradation is in a reticular-like pattern at the center of the cell. (x) Quantification of the percentage of cells degrading matrix after 8 hours. Results represent the mean +/− S.D. of >100 cells in each of three independent experiments. (y) Of the cells degrading matrix, the area of degradation was quantified and is normalized to the total cell area. Graphed results represent the mean +/− S.D. of 10 cells in each of three independent experiments. Note the reciprocal response in the tumor vs the stromal cells following Dyn2 KD. Scale bar, 10 μm. *p<0.05, **p<0.01.

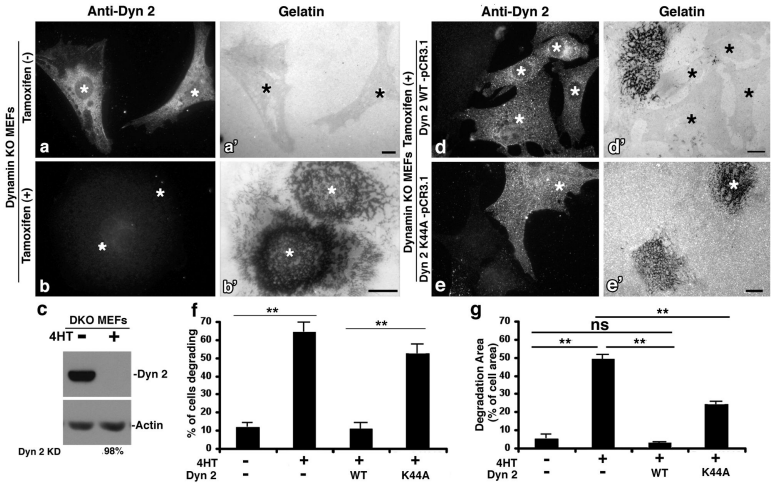

Figure 3. The substantial increase in degradation by Dynamin KO MEFs is reversed by Dynamin re-expression, and is dependent on its GTPase activity

A fibroblast cell line derived from an inducible Dyn1/2 genetic knockout (KO) model was analyzed for matrix degradation in the presence and absence of 4-hydroxy-tamoxifen (4HT) to induce dynamin knockout (DKO). (a, b) Parental [Tamoxifen (−)] or DKO [Tamoxifen (+)] MEFs plated on a fluorescent gelatin substrate were stained for Dyn2. Parental MEFs show substantial amounts of endogenous Dyn2, but exhibit almost no matrix degradation (a'). In contrast, DKO MEFs show a dramatic increase in matrix degradation with a characteristic reticular network pattern at the cell center (b'). (c) Western blot analysis of cells +/− tamoxifen treatment confirming Dyn2 knockout. The percent reduction in Dyn2 is shown. (d-e) Re-expression of Dyn2 in DKO MEFs results in a reversal of the degradation phenotype. Fluorescence images show re-expression of WT Dyn2 (d) or GTPase-deficient K44A Dyn2 (e) with corresponding degradation patterns on fluorescent gelatin (d'-e'). Note that the surrounding cells in which dynamin is not expressed degrade large amounts of matrix in comparison to the WT rescued cells (*) that degrade no matrix at all (d'). (f) Quantitation of the percentage of MEFs degrading matrix +/− DKO from three independent experiments, presented as the mean +/− S.D. Note that the Dyn2 K44A mutant-expressing cells continue to degrade matrix, indicating that the GTPase activity of Dyn2 is required to suppress degradation. Quantitative data represent the mean +/− S.D. of >100 cells in each of three independent experiments. (g) Of the cells degrading matrix, the area of degradation was quantified and normalized to the total cell area. Data represent the mean +/− S.D. of 10 cells per condition in each of three independent experiments. Bar, 10 μm. ** $p<0.01$.

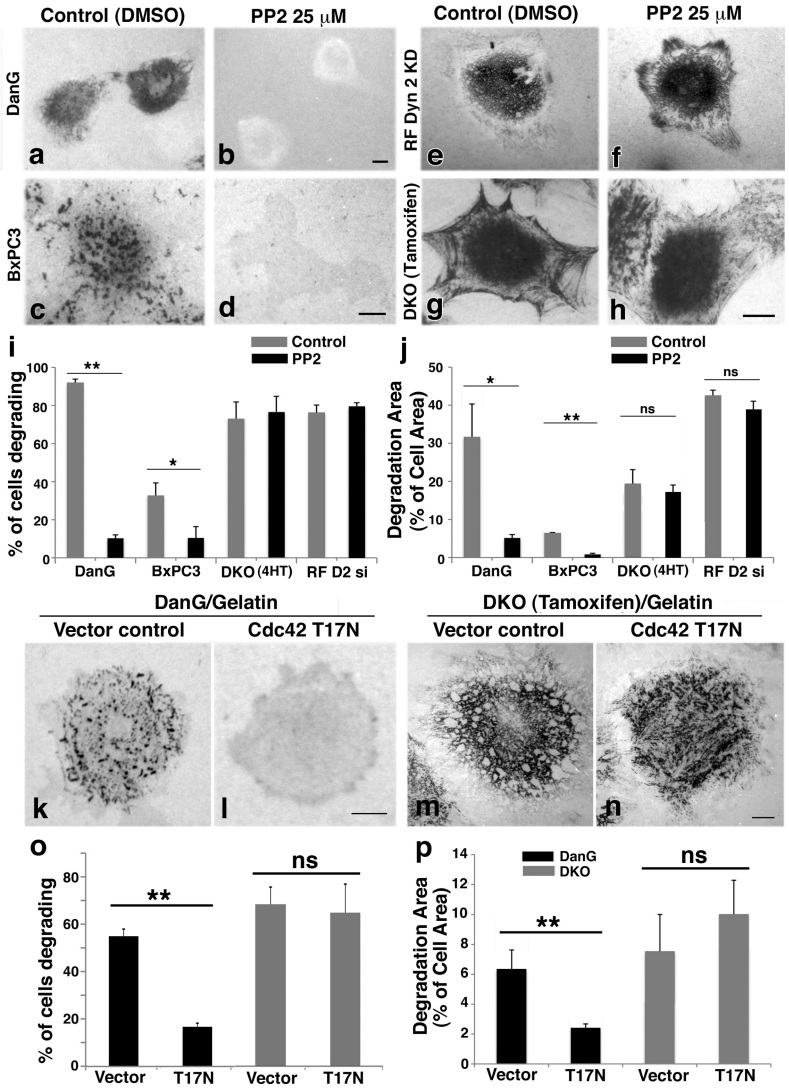

Figure 4. Matrix degradation by epithelial-derived tumor cells versus fibroblasts exhibits distinct requirements for Src kinase and Cdc42

(a-h) The indicated cell lines were plated on a fluorescent gelatin substrate in the presence of the MMP inhibitor BB-94. Following BB-94 washout, the cells were incubated +/− the Src inhibitor PP2 (25μM) for 8h. (a-d) Note that matrix degradation by the DanG and BxPC3 tumor cells is significantly reduced by Src inhibition. (e-h) Rat fibroblasts depleted of Dyn2 (RF Dyn2 KD) or Dynamin knockout MEFs (DKO) were plated on fluorescent gelatin as described above. In contrast to the tumor cells, both mesenchymal cell types continue to degrade large amounts of matrix, even under these high concentrations of PP2. (i) Quantification of the percentage of cells degrading matrix upon Src inhibition (n>100 cells per condition) or (j) the area of degradation per cell, normalized to total cell area, in matrix-degrading cells (n=10 cells per condition). (k-n) DanG tumor cells (k, l) or DKO MEFs (m, n) were transfected with dominant negative Cdc42 T174N and plated on fluorescent gelatin for 8h. Note that expression of Cdc42 T17N inhibits invadopodia-based matrix degradation by DanG cells, but not degradation by DKO MEFs. (o) Quantification of the percentage of cells degrading the matrix (n>50 cells per condition) and (p) the area of degradation per cell,

normalized to total cell area, in matrix-degrading cells (n≥10 cells per condition). All graphed data are represented as the mean +/− S.D. from three independent experiments.*p<0.05, **p<0.01.

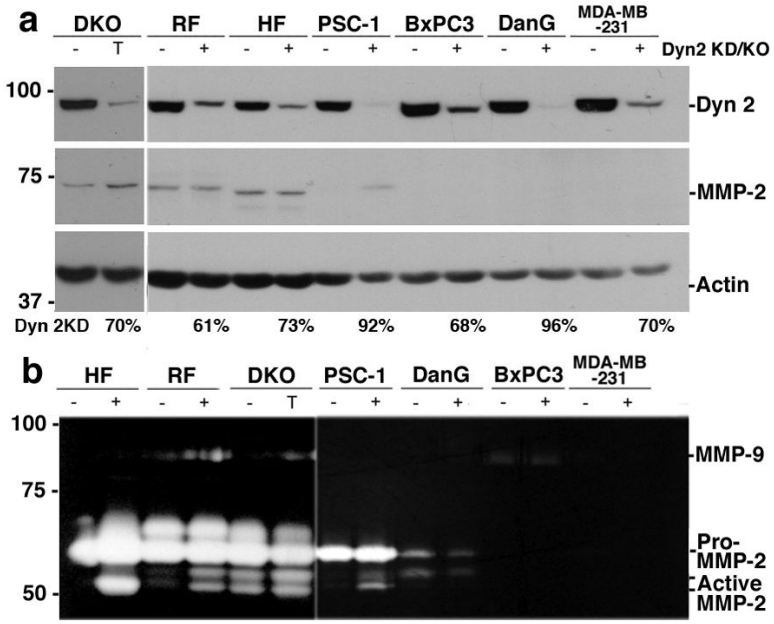

Figure 5. Differential expression and activation of the MMP-2 protease in stromal cells versus epithelial-derived tumor cells

(a) Western blot analysis of total MMP-2 protein levels in different mesenchymal and tumor cell lines following Dyn2 knockdown or knockout (T= tamoxifen-induced knockout). The percent knockdown of Dyn2 is included below the immunoblots. (b) Culture medium supernatant from the indicated cell lines was analyzed by zymography. Note the increase in gelatin degradation at the size of activated MMP-2 in fibroblasts and PSCs following depletion of Dyn2, while epithelial tumor cells show little or no MMP-2-based gelatin degradation. In both a and b, vertical white lines indicate regions where nonadjacent lanes were spliced together.

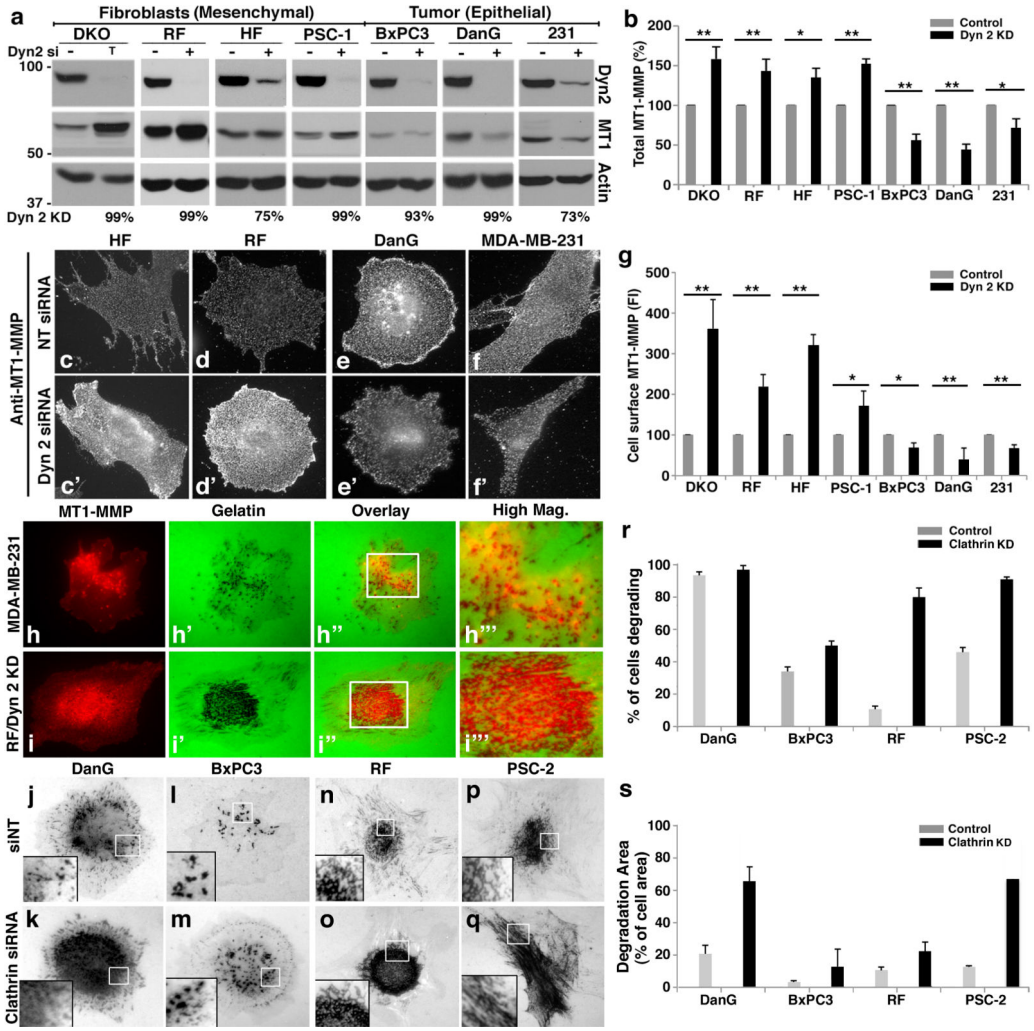

Figure 6. Reduction of Dyn2 causes an accumulation of MT1-MMP on the plasma membrane in stromal cells

(a) Western blot analysis of total MT1-MMP protein levels in mesenchymal and tumor cell lines following depletion of Dyn2 (T= tamoxifen induced knockout). White space indicates where blots were spliced. (b) Quantitation of three experiments shows an accumulation of MT1-MMP protein upon Dyn2 knockdown in mesenchymal cells, but not tumor cells. Results indicate the mean +/− S.D. of MT1-MMP levels, normalized to the control for each cell type. (c-f') Immunofluorescence staining of cell surface MT1-MMP with and without knockdown of Dyn2. Following Dyn2 depletion, fibroblasts showed a significant increase in surface MT1-MMP, while the tumor cells showed a modest reduction. (g) Quantification of cell surface MT1-MMP fluorescence intensity of each cell type +/− Dyn2 knockdown. Values were normalized to background fluorescence, and normalized to the control for each condition. Results represent the average+/− S.D. of >100 cells in each of three independent experiments. (h-i) Colocalization of MT1-MMP with areas of matrix degradation in both MDA-MB-231 tumor cells and rat fibroblasts that have been depleted of Dyn2. (j-q) Matrix degradation patterns of tumor or stromal cells that were depleted of clathrin by siRNA and plated on a fluorescent gelatin matrix. KD of clathrin increases degradation at tumor cell

invadopodia and at non-invadopodial sites in stromal cells. (r) The percent of cells degrading the matrix was scored (n>50 cells per condition, mean +/− S.D. from 2 independent experiments). (s) Of the cells degrading matrix, the area of matrix degradation was determined and normalized to the total cell area (n=10 cells per condition, mean +/− S.D. from 2 independent experiments). Bar, 10 μm. *p<0.05, **p<0.01.

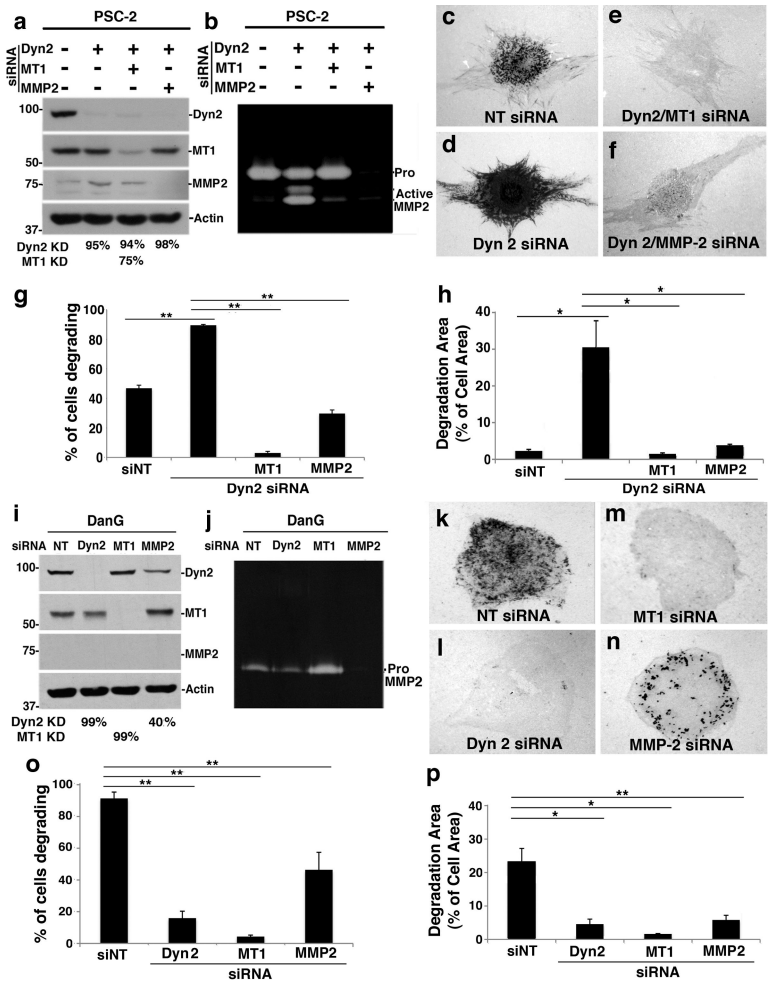

Figure 7. Non-invadopodial degradation requires MT1-MMP-stimulated MMP-2 activity

MT1-MMP (MT1), MMP-2, and Dyn2 were depleted by siRNA in PSCs or DanG tumor cells. The knockdowns were confirmed by western blot (a, i), and MMP-2 activity was assessed by zymography (b, j). (c-f) PSCs depleted of the indicated proteins were plated on fluorescent gelatin and matrix degradation was assessed after 8h. Knockdown of either MT1-MMP or MMP-2 inhibited the gelatin degradation in PSCs that was induced by loss of Dyn2. (k-n) In contrast, in DanG cells, invadopodial-based matrix degradation is blocked by siRNA-mediated depletion of either Dyn 2 or MT1-MMP, but is less affected by knockdown of MMP-2. (g, o) Quantitation of the percent of cells degrading the matrix (n>100 cells per condition), or (h, p) the area of degradation per cell, normalized to cell area, in matrix-degrading cells (n=10 cells per condition). Graphed data are shown as the mean +/− S.D. of three independent experiments. Bar=10 μm. **p<0.01.

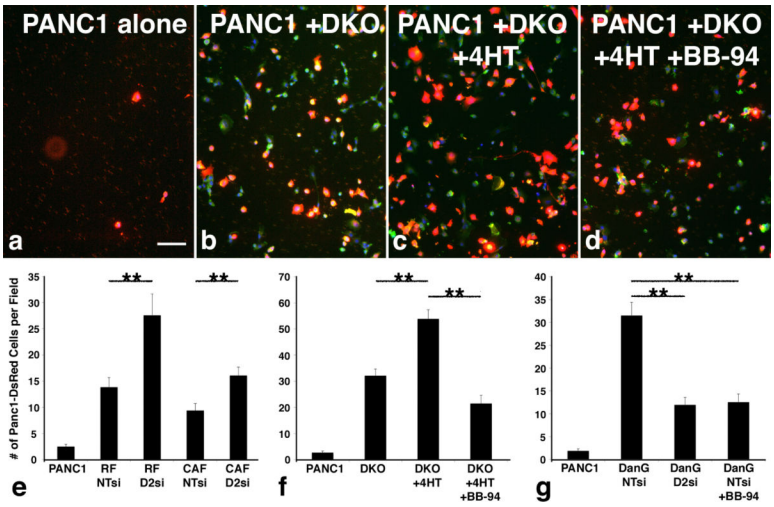

Figure 8. Matrix degrading fibroblasts accentuate the transwell invasion of tumor cells

PANC1 tumor cells, which do not degrade a gelatin matrix or invade across a transwell filter, were transduced to stably express mDsRed. The labeled PANC1 cells were cultured alone or co-cultured with stromal cells in a transwell invasion assay. (a-d) Representative images showing PDAC cells that have invaded across a gelatin-coated transwell membrane. PANC1 tumor cells were cultured individually (a), or co-cultured with parental DKO MEFs (b) or DKO MEFs treated with tamoxifen (4HT) to induce loss of Dyn2 (c). (d) Invasion was significantly reduced by the MMP inhibitor BB-94. All cells were labeled with FITC-Phalloidin (actin cytoskeleton) and DAPI (nuclei). (e-g) The number of PANC1 cells that invaded across the membrane was scored. (e) PANC1 were co-cultured with either rat fibroblasts (RF) or CAFs transfected with either a nontargeting siRNA or an siRNA targeting Dyn2. (f) PANC1 were co-cultured with parental DKO MEFs or DKO MEFs treated with tamoxifen to knock out Dyn1/2. Note that PANC1 tumor cells alone are unable to invade to the bottom of the transwell filter. This migration is increased upon the addition of control fibroblasts, an effect that is potentiated further upon the reduced expression of Dyn2. (g) PANC1 cells were co-cultured with DanG pancreatic tumor cells that were transfected with either a non-targeting siRNA or an siRNA targeting Dyn2. In the DanG tumor cells, note that reduction of Dyn2, which decreases matrix degradation, also decreases PANC1 invasion. In both (f) and (g), treatment with the MMP inhibitor BB-94 reduced invasion, showing that it is MMP-dependent. Graphed data represent the mean +/− S.E. of 13-15 10× fields over at least three independent experiments. Bar, 100μm. **p<0.01